

^{59}Co NMR Study of the Co States in Superconducting and Anhydrous CobaltatesI. R. Mukhamedshin,^{1,*} H. Alloul,^{1,†} G. Collin,² and N. Blanchard¹¹*Laboratoire de Physique des Solides, UMR 8502, Université Paris-Sud, 91405 Orsay, France*²*Laboratoire Léon Brillouin, CE Saclay, CEA-CNRS, 91191 Gif-sur-Yvette, France*

(Received 11 February 2005; published 20 June 2005)

^{59}Co NMR spectra in oriented powders of $\text{Na}_{0.35}\text{CoO}_2$ and in its hydrated superconducting (HSC) phase $\text{Na}_{0.35}\text{CoO}_2 \cdot 1.3\text{H}_2\text{O}$ reveal a single electronic Co state with identical T independent NMR shift tensor. These phases differ markedly from $\text{Na}_{0.7}\text{CoO}_2$, in which we resolve three types of Co sites. The large T variation of their spin susceptibilities χ^s and the anisotropy of the orbital susceptibility χ^{orb} allow us to conclude that charge disproportionation occurs in a nonmagnetic Co^{3+} and two magnetic sites with about 0.3 and 0.7 holes in the t_{2g} multiplet. The data are consistent with those for the single Co site in the anhydrous and HSC phase assuming the expected $\text{Co}^{3.65+}$ charge.

DOI: 10.1103/PhysRevLett.94.247602

PACS numbers: 75.20.Hr, 71.27.+a, 74.70.-b, 76.60.-k

The superconductivity (SC) induced by water insertion in $\text{Na}_{0.35}\text{CoO}_2$ [1] has led to the suggestion of an analogy with high T_c cuprates [2]. Indeed, metallic and magnetic states [3] occur in these layered transition metal oxides and the SC, which occurs for a limited range of carrier contents [4], might be explained by the magnetic scenarios proposed for the cuprates. The triangular lattice of the cobalt planes introduces a frustration of interactions between Co spins, which could be even more favorable than in the cuprates to the formation of exotic spin ground states [5]. Furthermore, cobaltates might display a richer variety of properties due to the two possible Co electronic configurations (Co^{3+} , $S = 0$ and Co^{4+} , $S = \frac{1}{2}$) in the high trigonal crystal field of the CoO_2 plane. A segregation into these 3^+ and 4^+ charges has been suggested [6] and would, for $x_0 \approx 0.7$, be linked with the atomic order of the Na layers [7]. This charge ordered metallic state, presumably responsible for the thermoelectric properties [8], should be physically quite distinct from the insulating charge and spin stripe order due to hole localization in some cuprates [9].

Prior to fully addressing these comparisons, it seems essential to perform atomic probe determination of the Co states all over the phase diagram. This issue is connected with that of the role of H_2O in inducing SC. While H_2O insertion should not *a priori* modify the electronic structure [10], it has recently been proposed [11,12] that $(\text{H}_3\text{O})^+$ ions increase the doping of the CoO_2 plane from 0.35 to 0.7, so that the electronic properties of the SC would be similar to those of the $x_0 \approx 0.7$ phase.

In the present work we use ^{59}Co NMR in oriented powders in order to probe the electronic properties of the Co sites. The analysis of the NMR shifts enables us to determine the orbital susceptibility χ^{orb} which is directly related to the charge state of the Co. We show for the first time [13] that three types of Co states occur in the x_0 phase at variance with the anticipated $\text{Co}^{3+}/\text{Co}^{4+}$ scenario [14]. On the contrary, the $x \approx 0.35$ sample is found to display a uniform $\text{Co}^{3.65+}$ charge state which is not modified upon water insertion. We therefore stress the contrast between the electronic properties on the two sides of the $x = 0.5$

composition. The large anisotropy of χ^{orb} found for the hole doped Co sites allows us to propose a scheme to reconcile the conflicting data [15,16] reported below T_c in the hydrated superconducting (HSC) samples, and to propose singlet SC. Our results open the way for experimental electronic characterization of the various magnetic states found for large Na content [17], and should stimulate realistic band structure calculations.

Two $x_0 \approx 0.7$ and the $x \approx 0.35$ samples were already used in Ref. [7]. Their NMR signals did not evolve for 18 months. A new x_0 sample with negligible Co_3O_4 content has been synthesized. A part of the $x \approx 0.35$ batch was hydrated into a HSC sample ($T_c = 3.9$ K) and its crystallite c axes were aligned in water in a 7 T applied field [18]. The sample was then frozen and kept below 0°C .

The $I = 7/2$ nuclear spin of ^{59}Co both senses the magnetic properties of the Co site and couples through its nuclear quadrupole moment Q to the electric field gradient (EFG) tensor $V_{\alpha\beta}$ created by its charge environment. The ^{59}Co NMR signal detected for $H \parallel c$ in the HSC sample is the most typical spectrum for a single site for which c is a principal axis of the EFG. It is reported in Fig. 1 as a recording versus H of the NMR spin echo intensity obtained with a $\frac{\pi}{2} - \tau - \frac{\pi}{2}$ pulse sequence. It displays a set of equally spaced peaks symmetrically arranged around the central $-\frac{1}{2} \leftrightarrow \frac{1}{2}$ transition. The frequency splitting $\nu_Q = 3eQV_{ZZ}/(h2I(2I - 1))$ is a measure of the EFG component V_{ZZ} with $Z \parallel c$. For $H \perp c$ the in plane ab axes of the crystallites are random in our samples, which results in a powder spectrum. The line shape reflects then the anisotropy $\eta = |(V_{YY} - V_{XX})/V_{ZZ}|$ of the in plane components of the EFG. The simulations of the spectra yield $\nu_Q = 4.103(10)$ MHz; $\eta = 0.22(2)$, in perfect agreement with NQR existing data [19]. The spectra for the anhydrous $x \approx 0.35$ sample are quite similar to that of the HSC sample. The small difference relates to slight discrete changes of ν_Q resolved only for $H \parallel c$. These can easily be attributed to EFG contributions of diverse local arrangements of Na^+ ions which are negligible in the SC samples due to the

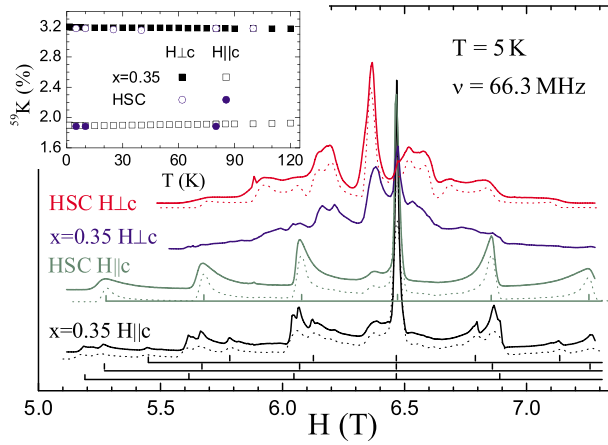


FIG. 1 (color online). ^{59}Co NMR spectra in the $x \approx 0.35$ samples. In the c direction, six out of the seven quadrupolar transitions are seen in this field sweep. Dotted lines are simulations with $\nu_Q = 4.1$ MHz and $\eta = 0.22$ (HSC sample) and $\nu_Q = 3.55, 4.17,$ and 4.45 MHz with intensity ratios 47/30/23 (anhydrous sample). Inset: T variation of the ^{59}Co NMR shifts.

larger Na^+ -Co distances upon water insertion. Remarkably, the spectra in the anhydrous sample display a unique central line for all Co sites. Furthermore, its anisotropic NMR shifts, which measure the local χ , are identical and nearly T independent in the two samples ($K_c = 1.9\%$ and $K_{ab} = 3.2\%$; see Fig. 1 and inset) [20]. This is strong evidence that the HSC and anhydrous samples display a quite identical uniformly charged state, e.g., $\text{Co}^{3.65+}$, with no resolvable difference in local χ , whatever the Na environment.

The situation is opposite for the spectra of the $x_0 \approx 0.7$ phase, which display many different Co sites [Fig. 2(b)] with distinct EFGs and magnetic shifts. To resolve the latter we took spectra with H tilted of $\theta = (\widehat{H}, \widehat{c})$, such that $3\cos^2\theta = 1$. For that “magic angle” (MA) the quadrupole satellites of the lines with $\eta = 0$ merge with their central lines, and the quadrupole spectra for $\eta \neq 0$ are also narrowed [Fig. 2(a)]. Besides the ^{23}Na signal one can easily distinguish then three Co sites, indexed with increasing shifts Co1, Co2, and Co3. The Co2 line has the largest broadening, to be associated hereafter with a large anisotropy of its NMR shift. In Fig. 2(a) we also show how we contrast the signals of these sites using their very distinct transverse spin-spin relaxation time T_2 . Indeed, a spin echo signal dies away for $\tau \gg T_2$, and for a short delay time (τ_S) the MA spectrum displays all sites, while for a long delay time (τ_L) only the Co1 and Na signals remain. This reveals that the signals of the “more magnetic” Co2 and Co3 sites have $T_2 < \tau_L$. Once the Co1 spectrum is determined with the (τ_L) data, it can be rescaled and deduced from the (τ_S) spectrum to isolate the Co2 and Co3 signals [“Diff” in Fig. 2(a)].

This procedure has been quite powerful in resolving the spectra for any θ as exemplified for $H \parallel c$ in Figs. 2(b) and

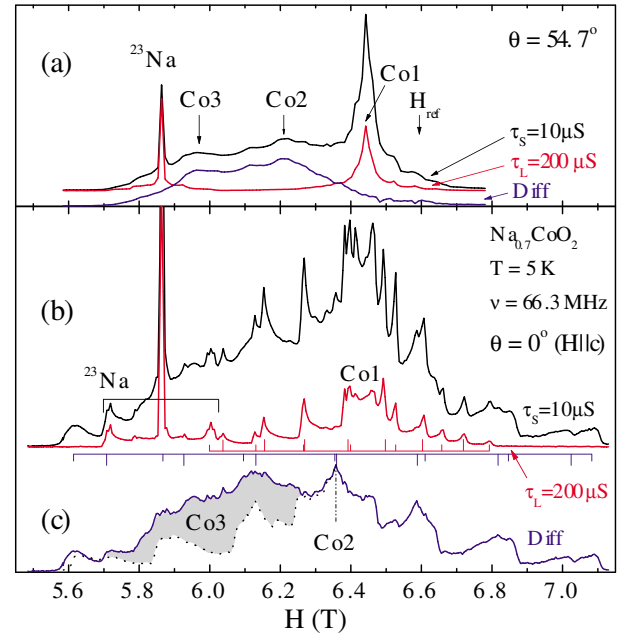


FIG. 2 (color online). ^{59}Co NMR spectra taken as the H dependence of the spin echo taken for short (τ_S) or long (τ_L) delay between pulses. Upper part: (a) For H tilted at the “magic angle” θ . Lower part: (b) For $H \parallel c$ the (τ_L) spectrum corresponds to the Co1a and Co1b sites. (c) The difference spectrum reveals the short T_2 sites Co2a, Co2b, and Co3. The quadrupole satellites of the Co1 and Co2 sites are marked by ticks.

2(c). The τ_L signal for Co1 is seen to display more than seven well resolved quadrupolar lines, and a full analysis reveals that it consists of the superposition of spectra of two sites Co1a and Co1b with similar shifts $\nu_{Q1a} = 1.19(1)$ and $\nu_{Q1b} = 1.38(1)$ MHz. The difference spectrum of Co2 and Co3 in Fig. 2(c) reveals that Co2 consists of two sites Co2a and Co2b with $\nu_{Q2a} = 2.18(2)$ and $\nu_{Q2b} = 1.55(2)$ MHz. The highly shifted Co3 component appears on top of the simulated Co2 spectrum. Here Figs. 2(b) and 2(c) have been displayed to visualize the method used, but a full analysis required a collective treatment of more than 50 spectra taken at different T and H . We postpone the details on the EFG data to a full technical report and focus hereafter on the magnetic information extracted from the NMR shifts.

Large T variations of ^{59}Co NMR shifts, which reflect the anomalous magnetism of the CoO_2 planes [7], were detected in all cases except for the Co1 sites for $H \perp c$, as reported in Fig. 3(a). For this reason, this signal had been attributed to nonmagnetic Co^{3+} in Ref. [6]. For $H \parallel c$ the Co1 and Co2 sites exhibit a similar increase of K_c with decreasing T , much smaller than for Co3. For $H \perp c$ the powder spectrum of Co2 similar to that of the HSC sample of Fig. 1 is harder to resolve, so the anisotropy of the Co2 and Co3 shifts could be obtained by comparing K_c to the isotropic $K_{\text{iso}} = \sum K_\alpha/3$ obtained from MA spectra.

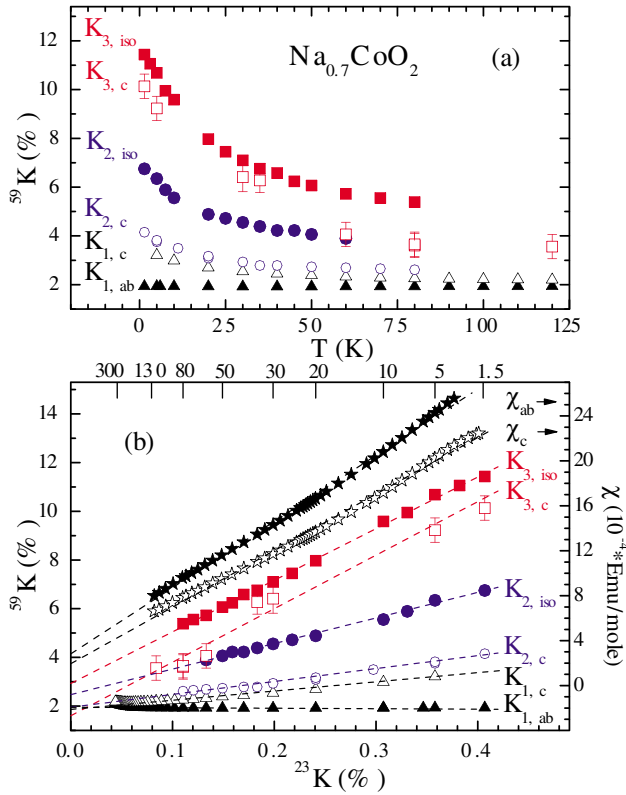


FIG. 3 (color online). (a) T variation of the shifts $K_{i,\alpha}$ of the Co sites. $K_{i,iso}$ are taken from MA spectra. (b) NMR shift data for the various Co sites (left scale) and SQUID data for χ_{α}^m (right scale) are plotted versus the ^{23}Na NMR shift (Fig. 4 in Ref. [7]).

The macroscopic susceptibility taken in a direction α ,

$$\chi_{\alpha}^m = \chi^{\text{dia}} + \chi_{\alpha}^{\text{orb}} + \chi_{\alpha}^s = \chi^{\text{dia}} + \sum_i [\chi_{i,\alpha}^{\text{orb}} + \chi_{i,\alpha}^s(T)],$$

involves the diamagnetism of the ion cores and the orbital and spin terms split in their $\text{Co}(i)$ sites' components. The NMR shifts of sites i are linked to the χ 's through specific hyperfine couplings A ,

$$K_{i,\alpha} = K_{i,\alpha}^s + K_{i,\alpha}^{\text{orb}} = A_{i,\alpha}^s \chi_{i,\alpha}^s(T) + A_{i,\alpha}^{\text{orb}} \chi_{i,\alpha}^{\text{orb}}.$$

The ^{59}Co diamagnetic shift contribution is included in Ref. [20]. As the ^{23}Na shift [7] is purely due to the T dependent spin term, it is essential to compare $^{59}K_{i,\alpha}$ to $^{23}K_{i,iso}$. As can be seen in Fig. 3(b) a linear dependence is found for all sites below 120 K when the Na motion is frozen. So these data confirm that all Co pertain to the same phase in which a single T variation characterizes the local $\chi_{i,\alpha}^s(T)$. The slopes of the linear fits give the relative magnitude of the spin contributions $K_{i,\alpha}^s/^{23}K$, while their $^{23}K = 0$ intercepts give the estimates of the Co orbital NMR shifts $K_{i,\alpha}^{\text{orb}}$ reported in Table I. For comparison, SQUID data for $\chi_{\alpha}^m(T)$ taken in $H = 5$ T for our oriented sample with minimal Co_3O_4 content, also plotted in Fig. 3(b) versus ^{23}K , confirm this unique T dependence.

TABLE I. NMR parameters for the 3 magnetically distinct sites for the samples with $x_0 \approx 0.70$.

Site	$I_i(\%)^a$	$K_{i,iso}^{\text{orb}}(\%)$	$K_{i,iso}^s/^{23}K$	$K_c^{\text{orb}}(\%)$	$K_c^s/^{23}K$
Co1	26(4)	1.89(2)	2.44(8)	1.95(1)	3.8(1)
Co2	55(5)	2.5(1)	10.5(3)	1.94(5)	5.1(2)
Co3	19(4)	2.9(1)	21.2(2)	1.6(4)	22(2)

^aAll ^{59}Co nuclei being detected in the anhydrous $x \approx 0.35$ sample, its central line intensity $I_{(0.35)}$ was used to calibrate the Co1 central line intensity. The ratio $I_1/I_{(0.35)} = 0.22(3)$ found ensures that all Co are detected as well in the $x_0 \approx 0.7$ phase within experimental accuracy.

These data allow us to separate $\chi_{\alpha}^s(T)$ from $(\chi^{\text{dia}} + \chi_{\alpha}^{\text{orb}})$, the latter being the extrapolation to $K = ^{23}0$. With tabulated values we calculate for $\text{Na}_{0.7}\text{CoO}_2$ $\chi^{\text{dia}} = -0.35$ and then $\chi_{ab}^{\text{orb}} = 3.1(2)$ and $\chi_c^{\text{orb}} = 2.3(2)$, in 10^{-4} emu/mole units [21].

This anisotropy of orbital χ , seen on both the macroscopic $\chi_{\alpha}^{\text{orb}}$ and the local $K_{i,\alpha}^{\text{orb}}$, being mainly of ionic origin, gives us an insight on the ionic states of the Co sites. For a Co^{3+} ionic state, the lower energy t_{2g} triplet levels are filled and the ionic shell has a spherical symmetry, so that $\chi^{\text{orb}} = 2\mu_B^2/\Delta$ is isotropic. Here Δ is the $t_{2g} - e_g$ energy splitting. Holes introduced on the t_{2g} levels yield modifications of $\chi_{i,\alpha}^{\text{orb}}$ that depend on the spatial direction of the populated hole orbitals. Therefore the isotropy of $K_{1,\alpha}^{\text{orb}}$ allows us to assign Co^{3+} to the Co1 site, while the anisotropic values of $K_{2,\alpha}^{\text{orb}}$ and $K_{3,\alpha}^{\text{orb}}$ imply that Co2 and Co3 have hole contents x_i , to be estimated from our data. A first relation between the x_i is given, for $x_0 \approx 0.7$, by the charge neutrality condition $0.55x_2 + 0.19x_3 = 0.3$, using the fractional occupancies I_i of the Co sites given in Table I. With the rough but sensible assumption that the orbital anisotropy scales with the hole content x_i , we obtain $x_2/x_3 \approx 0.44$ from the data for $K_{i,iso}^{\text{orb}}/K_{i,c}^{\text{orb}}$ listed in Table I, which results in charge states $\text{Co}^{+3.3(1)}$ and $\text{Co}^{+3.7(1)}$, respectively, for Co2 and Co3.

In the light of these results we may now reexamine the anisotropic ^{59}Co shift data found above in the $x \approx 0.35$ samples. As the 0.65 hole content of the t_{2g} orbital in the latter samples is similar to that estimated for the Co3 site, we might expect similar orbital shifts $K_c = 1.6(4)\%$, $K_{i,iso}^{\text{orb}} \approx 2.9(1)\%$, that is, $K_{ab}^{\text{orb}} \approx 3.5(4)\%$. These values are remarkably close to the total shifts $K_c = 1.9\%$, $K_{ab} = 3.2\%$, reported in Fig. 1 in the HSC sample, in which case the spin shifts K_{α}^s are then quite small in the HSC samples. In case of singlet SC the K_{α}^s are expected to decrease below T_c and to vanish at $T = 0$. Two conflicting reports indicate (i) a decrease from $K = 3.2\%$ to 2.7% [15] suggesting singlet SC and (ii) no variation of $K = 1.9\%$ [16] pointing towards triplet SC. From our normal state data, it is clear that the authors of (i) and (ii) monitored, respectively, the $H \perp c$ and the $H \parallel c$ central line singularities in partially oriented samples and the two sets of data are reconciled if

the spin shifts are $K_{ab}^s \approx 0.5\%$ and $K_c^s \approx 0$. The latter would be consistent with our observation (see Table I) that $K_{i,c}^{\text{orb}} \approx 1.9\%$ is nearly independent of the charge state of the Co. The overall consistency is therefore in favor of the arguments of (i) for spin singlet SC. To conclude on the properties of the HSC phase, we have also demonstrated here that water insertion does not modify the electronic properties for $x \approx 0.35$, which contradicts recent proposals [11,12]. Therefore, the absence of SC in the anhydrous sample could result from a depression of T_c induced by the Na^+ ion disorder. Even if present in the HSC samples one can anticipate that such a disorder would be screened by the water layers and be less felt by the CoO_2 plane carriers.

As for the $x_0 \approx 0.70$ sample we have demonstrated that the fraction of Co^{3+} is quite small, which totally discards the purely ionic $\text{Co}^{3+}/\text{Co}^{4+}$ picture, which would presumably yield a Mott Hubbard insulating state. Our results allow us to establish that extracting Na^+ from NaCoO_2 leads rather to delocalized states on specific Co sites, while only a few Co sites remain Co^{3+} . This evidence for partial hole filling on Co2 and Co3 sites is more compatible with a metallic state, such as a commensurate CDW state, although a nearly localized behavior is still required to explain the drastic T variation of the local χ . We have emphasized here the different magnetic characters of the Co sites through the modifications of $K_{i,\alpha}^{\text{orb}}$. The spin shifts $K_{i,\alpha}^s$ do also probe the local magnetism and the fact that $K_{i,\text{iso}}^s/^{23}K_{\text{iso}}^s$ is small (≈ 2.3) for Co1 and increases to ≈ 10 and ≈ 20 for Co2 and Co3 is in perfect qualitative agreement with an increase of hole content on the t_{2g} multiplet for these sites. However, a nuclear spin is coupled both to its own electron orbitals giving an on-site hyperfine field (HF) and to its nearest neighbors (transferred HF). So, further analysis of the $K_{i,\alpha}^s$ data requires a knowledge of the arrangement of the differently charged Co sites to undertake electronic structure estimates of the hyperfine couplings $A_{i,\alpha}^s$. Although the EFG's and the site occupancies will help in this process, special care is presently devoted to secure first the atomic structure through x rays and neutron investigations, since it is clear that the atomic arrangement of Na is correlated to that of the Co charges.

It is often soundly suggested that the Na1 which sits on top of the Co atoms stabilize the less positively charged Co^{3+} , so that the role of the Na order could be essential for the physics of the $x \geq 0.5$ phases. The fact that large high T Curie-Weiss dependencies occur quite generally for $x > 0.5$ might as well indicate that magnetism is an incipient property of the CoO_2 planes with sufficient hole doping on the Co. The subtle Na ordering could also play a second, more marginal 3D role, by favoring c axis couplings between hole doped magnetic Co ions, which might explain the diverse low T ordered magnetic states [17] found for $x > 0.75$. The methods used here to determine the Co states might apply for other Na ordered phases and should help to resolve these issues. We have demonstrated here

that magnetic models should not consider all Co sites on the same footing and that Na_xCoO_2 are not simple realizations of Heisenberg spin Hamiltonians. Finally, it is, of course, obvious that our mainly ionic approach can only be qualitative, as we are dealing with an original organization of Co charges in a strongly correlated band in which carriers avoid some sites. Further progress will have to await realistic band structure calculations taking into account the correlations, which could reproduce both charge disproportionation and anomalous magnetism.

We acknowledge J. Bobroff and P. Mendels for their help on the experimental setup, for stimulating discussions, and for their careful reading of the manuscript.

*Permanent address: Physics Department, Kazan State University, 420008 Kazan, Russia.

†Electronic address: alloul@lps.u-psud.fr

- [1] K. Takada *et al.*, Nature (London) **422**, 53 (2003).
- [2] G. Baskaran, Phys. Rev. Lett. **91**, 097003 (2003).
- [3] J. Sugiyama *et al.*, Phys. Rev. Lett. **92**, 017602 (2004).
- [4] R.E. Schaak, T. Klimczuk, M.L. Foo, and R.J. Cava, Nature (London) **424**, 527 (2003).
- [5] B. Kumar and B.S. Shastry, Phys. Rev. B **68**, 104508 (2003).
- [6] R. Ray, A. Ghoshray, K. Ghoshray, and S. Nakamura, Phys. Rev. B **59**, 9454 (1999).
- [7] I.R. Mukhamedshin, H. Alloul, G. Collin, and N. Blanchard, Phys. Rev. Lett. **93**, 167601 (2004).
- [8] I. Terasaki, Y. Sasago, and K. Uchinokura, Phys. Rev. B **56**, R12 685 (1997).
- [9] J.M. Tranquada *et al.*, Nature (London) **375**, 561 (1995).
- [10] M.D. Johannes and D.J. Singh, Phys. Rev. B **70**, 014507 (2004).
- [11] K. Takada *et al.*, J. Mater. Chem. **14**, 1448 (2004).
- [12] C.J. Milne *et al.*, Phys. Rev. Lett. **93**, 247007 (2004).
- [13] F.L. Ning, T. Imai, B. W. Statt, and F.C. Chou, Phys. Rev. Lett. **93**, 237201 (2004). These authors detected two Co signals for various Na contents, but did only a limited study of their 0.67 phase, which looks similar to ours.
- [14] K.-W. Lee, J. Kunes, and W.E. Pickett, Phys. Rev. B **70**, 045104 (2004).
- [15] Y. Kobayashi, M. Yokoi, and M. Sato, J. Phys. Soc. Jpn. **72**, 2453 (2003).
- [16] M. Kato *et al.*, cond-mat/0306036.
- [17] P. Mendels *et al.*, Phys. Rev. Lett. **94**, 136403 (2005).
- [18] A. V. Egorov *et al.*, Sov. Phys. JETP **70**, 658 (1990).
- [19] T. Fujimoto *et al.*, Phys. Rev. Lett. **92**, 047004 (2004).
- [20] The ^{59}Co reference frequency used is 10.054 MHz/T.
- [21] These extrapolated SQUID data exceed by about 10^{-4} emu/mole the values $\chi_{ab}^{\text{orb}} = 1.79$ and $\chi_c^{\text{orb}} = 1.25$ (10^{-4} emu/mole), which can be estimated from the data for $K_{i,\alpha}^{\text{orb}}$ and I_i of Table I, assuming a single value for $A_{i,\alpha}^{\text{orb}}$ whatever the 3d orbital, i.e., $A^{\text{orb}} = 2\langle r^{-3} \rangle = 13.4$ a.u., from Ref. [6]. Experimental inaccuracies in the extrapolations and the rough above assumption might explain this 50% difference.